

Article

Exploring Spectral Uncertainty on the Surface of Brass Samples by Laser-Induced Breakdown Spectroscopy

Wei Wang ^{1,*} , Lanxiang Sun ² and Faquan Li ¹

¹ State Key Laboratory of Magnetic Resonance and Atomic and Molecular Physics, Innovation Academy for Precision Measurement Science and Technology, Chinese Academy of Sciences, Wuhan 430071, China; lifaquan@apm.ac.cn

² Shenyang Institute of Automation, Chinese Academy of Sciences, Shenyang 110016, China; sunlanxiang@sia.cn

* Correspondence: wangwei@apm.ac.cn; Tel.: +86-02787198037

Abstract: The shot-to-shot measurement uncertainty restricts the application of laser-induced breakdown spectroscopy (LIBS) technically, to a certain extent. In order to further deepen the understanding of spectral stability, in this paper, the effects of the laser's focus depth, the delay of the spectrometer, and the position of the spectrum collection on the spectral stability were carefully researched. Moreover, the dynamic characteristics of plasma were studied at different laser focusing depths. Research has found that the morphological changes of plasma are relatively stable, without significant changes, despite varying depths of laser focus on the sample surface. In addition, it was found that stable elemental emission spectra can always be obtained in the early plasma aggregation region.

Keywords: laser-induced breakdown spectroscopy; LIBS; plasma



Citation: Wang, W.; Sun, L.; Li, F. Exploring Spectral Uncertainty on the Surface of Brass Samples by Laser-Induced Breakdown Spectroscopy. *Chemosensors* **2024**, *12*, 49. <https://doi.org/10.3390/chemosensors12030049>

Received: 19 February 2024

Revised: 13 March 2024

Accepted: 18 March 2024

Published: 19 March 2024



Copyright: © 2024 by the authors. Licensee MDPI, Basel, Switzerland. This article is an open access article distributed under the terms and conditions of the Creative Commons Attribution (CC BY) license (<https://creativecommons.org/licenses/by/4.0/>).

1. Introduction

Compared with other technologies, laser-induced breakdown spectroscopy (LIBS) has attracted widespread attention due to its advantages, such as fast analysis speed, high degree of automation, no complicated sample preparation, and simultaneous online analysis of multiple elements [1–5]. However, due to the uncertainty of the collected spectral intensity, accurate quantitative analysis of LIBS in industrial applications becomes extremely difficult [6–8].

In order to identify the root cause of spectral uncertainty, many researchers have performed a lot of work. Rosalie A. Multari et al. [9] presented a detailed study of the sampling geometry on elemental emissions in LIBS and their effects on analytical results. It was found that plasma temperature, mass of ablated material and atomic emission intensities depend strongly on the lens-to-sample distance. Richard Wisbrun et al. [10] found that factors such as laser intensities, sample surface humidity, crater formation, aerosol production and spectrometer delay will affect the detection limits and the quality of the analysis of environmental samples (soil, sand, etc.). Moreover, J.A. Aguilera et al. [11] discussed the variation of emission line intensities of laser-induced plasmas with the laser pulse energy and the lens-to-sample distance. They reported that under different pulse energy, a focusing position at which the maximum line emission and the lower RSD of absolute intensity are produced. S. S. Harilal et al. [12] studied the expansion behavior of the plasma at different ambient air pressures ranging from 10^{-6} to 100 Torr, they found that when the ambient pressure is lower than 0.01 Torr, the plasma expands freely. Moreover, Sy-Bor Wen et al. [13,14] discussed that for ablation in a gas with higher atomic mass (e.g., Ar and Ne) the vapor plume expanded more slowly a few nanoseconds after the start of the laser pulse, compared to that in a lower atomic mass (e.g., He). Moreover, Yang-Ting Fu et al. [15,16] analyzed a titanium alloy sample when the focal length of the lens was 150 mm and the depth of focus of the laser on the sample surface was 2 mm, they assumed

that the observed total number density fluctuation by the optical system caused by plasma morphology variation is main factor that affects the LIBS signal repeatability.

To enhance comprehension of the factors contributing to spectral uncertainty, this paper meticulously investigates the impact of laser focus depth, spectrometer delay, and spectrum collection position on spectral stability. Additionally, the dynamic properties of plasma were examined across varying laser focus depths. Through an analysis of plasma evolution characteristics and observed spectral stability, preliminary conclusions regarding the method for attaining a stable plasma emission spectrum signal on a brass sample are presented.

2. Materials and Methods

The experimental setup is shown in Figure 1. An Ultra Bigsky laser (1064 nm, 15 ns) was employed as the laser source. The laser beam initially traverses a beam shaper, featuring a 1:1.5 expansion ratio, to reduce the divergence angle of the beam. Subsequently, it traverses an energy attenuator consisting of a half-wave plate and a polarizer. Finally, the laser beam focuses on the sample surface by passing through a lens with a focal length of 50 mm. The energy of laser focusing on the surface of the sample is 95 mJ, and the energy standard deviation of 100 laser pulses is 1.1. A 15 mm focal length lens is employed to couple the plasma emission beam into a fiber. The optical fiber used has a core diameter of 600 μm . The plasma emission spectrum is detected using a spectrometer consisting of ME-5000 and Andor's intensified charge-coupled device (ICCD) camera. The spectrometer's shutter opening time (TTL width) is set to 3 μs and a gain (MCP gain) of 2500. For investigating the time evolution characteristics of the plasma, the ICCD camera is also utilized to capture plasma topography. Additionally, a trigger (DG645, Stanford Research System, Palo Alto, CA, USA) is employed to control the relative delay time between the laser and the ICCD camera.

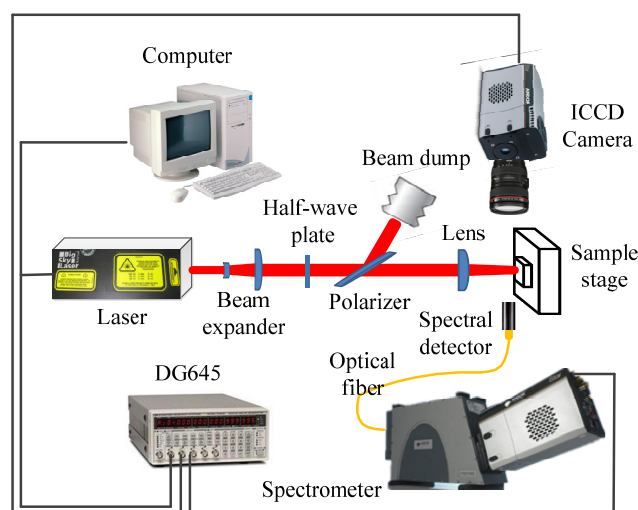


Figure 1. Experimental setup.

The experimental sample is a brass sample containing 95.9% copper (Cu) and 4.02% zinc (Zn). The laser is utilized to irradiate each sampling point on the sample surface 80 times. The initial 10 pulses are employed for sample cleaning, and the spectrum corresponding to the remaining 70 pulses is utilized for analysis. Experiments have studied the fluctuation characteristics of the plasma emission spectra under different laser focus depth, different collection positions and different spectrometer delays. When the laser focus is above the sample, the laser defocus is positive, and when the focus is below the sample, the laser defocus is negative. The laser defocus adjustment range is $-4\text{ mm}\sim 4\text{ mm}$, with an interval of 1 mm. The position of the spectrum collection position is performed at 1–5 positions as shown in Figure 2, each with a difference of 1 mm. Moreover, the relative

laser delay of the spectrometer was set to 1 μs , 5 μs , 10 μs , 20 μs , and 30 μs to study the plasma emission spectrum characteristics at different moments.

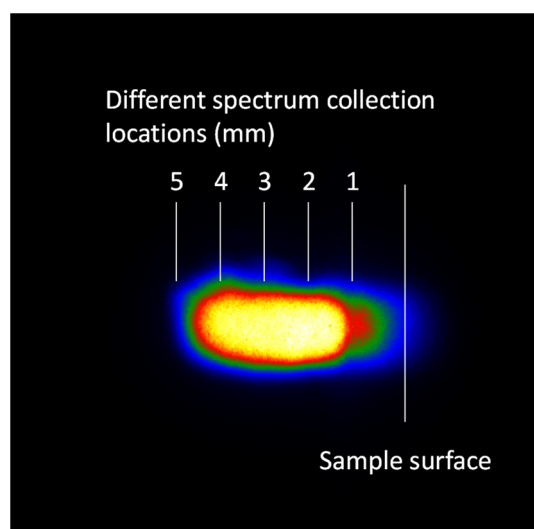


Figure 2. Different spectrum collection locations.

3. Results and Discussion

3.1. Spectrometer Delay and Spectral Stability

When high-energy laser pulses interact with the sample, atoms and molecules within the sample become excited, resulting in the formation of a high-temperature, high-density plasma. Particles within the plasma, possessing elevated energy levels, emit characteristic spectral signals upon returning to their ground state. Closely associated with this process is the collection delay of the spectrometer, which is the time from the emission of the laser pulse to the initiation of spectrum collection for the plasma emission. Due to the relatively short lifetime of the laser-induced plasma, the precise selection of the spectrometer's collection delay is directly related to the timing of interactions, such as the laser pulse with the sample, the plasma with the sample, and the plasma with the surrounding gas. Both excessively short or long delays may influence the incomplete formation or premature diffusion of the collected plasma emission spectrum region, consequently directly impacting the intensity, stability, and shape of the spectral signal [2,3,17].

To examine spectral stability as the plasma evolves, this study investigates the relationship between spectral intensity and stability under varying acquisition delays, while keeping the laser focal depth at 0 mm and aligning the spectral acquisition position with position 2 in Figure 2. As shown in Figure 3, at a spectrometer delay of 1 μs , the collected spectral lines exhibit strong and stable intensity. The standard deviation for the single spectrum of O 777.42 nm is within 5%. However, with a spectrometer delay of 5 μs , the relative standard deviation (RSD) of the single spectrum increases to about 10% for matrix elements (Cu and Zn) and air elements (N, H, and O). In addition, as the laser delay continues to increase, two trends emerge. Firstly, the intensity of the spectrum signal collected by the spectrometer weakens. Secondly, the spectrum stability experiences a sharp decline.

As shown in Figure 4, plasma patterns were captured under different laser delays. From this Figure, it can be seen that the plasma morphology differences captured under the same delay in the early stages were relatively small. The initial morphology of the plasma is relatively stable. During the period of 200 ns to 10 μs , the obtained plasma morphology is relatively stable. Due to diffusion and ablation, there are significant differences in the morphology of plasma at the same delay in the later stage. At 20–40 μs , the differences in plasma morphology captured at the same time become increasingly significant. Moreover, as a result of plasma shock waves, a distinct trend was observed wherein the plasma moved in the opposite direction of the laser.

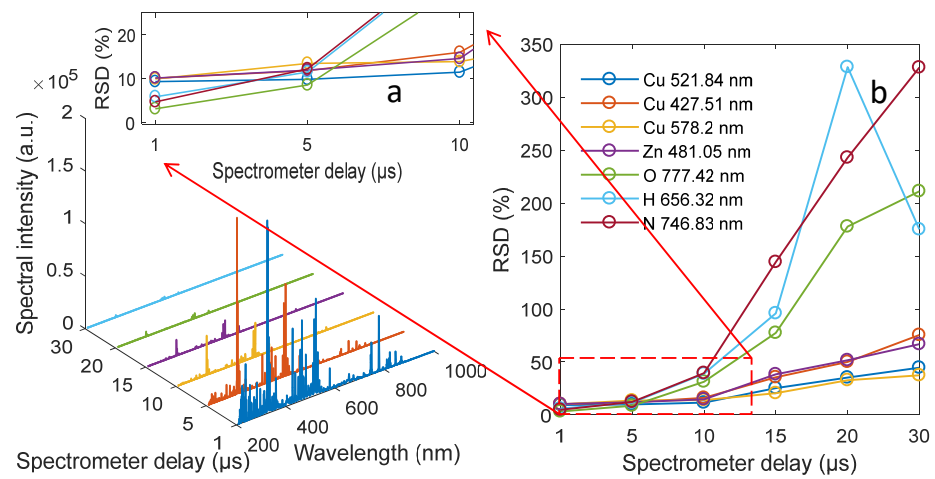


Figure 3. The variation in the spectral stability with the delay of the spectrometer. Figures (a) and (b) respectively show the variation of the collected spectra and the relative standard deviation of spectral line intensity with the delay of the spectrometer.

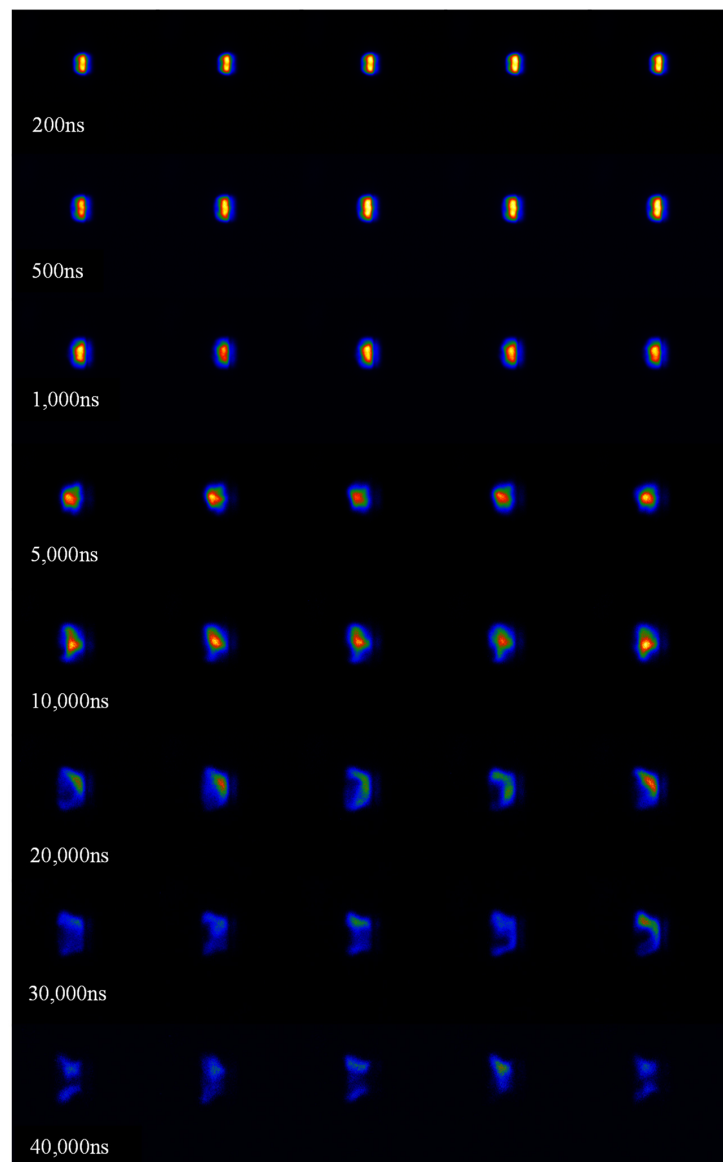


Figure 4. Fluctuations in plasma morphology.

Considering the spectrometer's integration time is $3 \mu\text{s}$ and the stability of the generated plasma emission spectrum, this phenomenon indicates that within $1\text{--}4 \mu\text{s}$ after the laser is generated, the number of luminescent particles in the collected signal region of the plasma remains relatively constant. However, as the collection delay increases, the collected spectra show weakened intensity and decreased stability, as shown in Figure 3a,b, respectively. The reason for this phenomenon was that as the collection delay increases, the number of particles in the spectral collection area decreased and the fluctuation increased.

From Figure 5b, it can be seen that when the spectral acquisition delay is $1 \mu\text{s}$, the relative standard deviation of the collected spectral lines for the three elements C, H, and O is about 5%. For the spectral lines of Cu and Zn, the relative standard deviation of the collected spectral lines is about 10%. When the delay of the spectrometer is $5 \mu\text{s}$, the relative standard deviations of the spectral lines of C, H, O, Cu, and Zn are all about 10%. However, when the delay of the spectrometer exceeds $10 \mu\text{s}$, the relative standard deviation of the spectral line intensities corresponding to C, H, and O suddenly increases, even exceeding 100%, while the trend of the relative standard deviation of the spectral lines for Cu and Zn is not very obvious. The observed phenomenon may be attributed to the fact that when the collection delay of the spectrometer exceeds $10 \mu\text{s}$, the spectral signal emitted by air particles gradually becomes submerged in the spectral background.

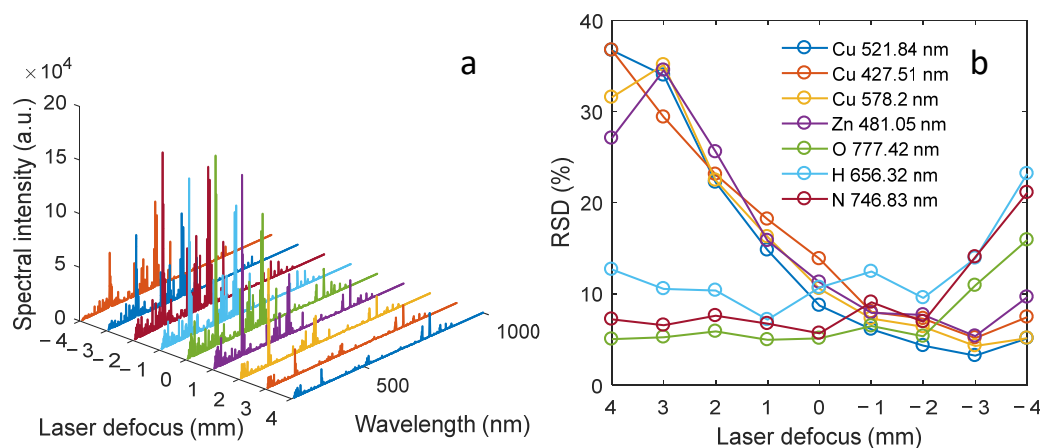


Figure 5. Spectral intensity and relative standard deviation under different laser defocus. Figures (a) and (b) respectively show the variation of the collected spectra and the relative standard deviation of spectral line intensity with the laser defocus.

3.2. Laser Defocus and Spectral Stability

The different focusing depths of the laser on the sample surface will lead to inconsistent power density of the laser on the sample surface, directly affecting the interaction process between the laser and the sample. Appropriate focusing depth helps to ensure that the laser pulse can fully excite the elements in the sample, generating stable plasma emission signals. Focusing too shallow or too deep may lead to incomplete plasma formation or interaction with the surrounding environment, thereby affecting the stability of spectral signals [18].

In this study, when the spectrometer's delay time is set to $1 \mu\text{s}$ and the spectrum collection position is 1 as indicated in Figure 2, spectral collection is carried out. In order to ensure that the spectral acquisition position remained unchanged relative to the sample surface, the spectral acquisition device moved simultaneously with the sample surface when adjusting the focusing depth of the laser on the sample surface. The relationship between spectral stability and the depth of laser focus on the sample surface has been studied.

The obtained spectrum intensity under different defocus conditions are shown in Figure 5a. The variation of the relative standard deviation of the seven spectral lines of the selected Cu, Zn, O, H and N elements with the laser defocusing amount is shown in Figure 5b.

From Figure 5a, when the laser focusing depth is between -4 mm and 1 mm, the overall intensity of the collected spectra is basically consistent. When the laser focusing depth is between $2\sim 4$ mm, the spectral intensity values show a gradually decreasing trend. When the defocus of the laser is 4 mm, most of the energy is used to break down the air. Due to the higher breakdown threshold of the air sample compared to brass, and the relatively low air density, the total density of luminescent particles in the plasma decreases, resulting in a relatively weak spectral intensity collected. As the defocus of the laser decreases, more and more energy is used to excite the surface material of the sample, and increases the overall density of luminescent particles in the plasma, ultimately resulting in a stronger spectral intensity collected.

Figure 5b shows the fluctuation of the relative standard deviation of the seven selected spectral lines with the defocusing amount of the laser. For the spectral line intensities of the three elements of O, H and N, the spectral intensity is relatively stable when the laser defocus is changed between -2 and 4 mm. However, the stability of the three spectra of N, H and O decreases when the laser defocusing distance changes from -2 to -4 mm. As for the spectral line of Cu and Zn in brass, the stability of spectral line is enhanced with the decrease in laser defocusing. The relative standard deviation of spectral lines can be reduced from above 35% to less than 10% .

The reason for this phenomenon may be that as the defocusing amount of the laser gradually decreases, more and more laser energy is used to excite the surface of the sample, resulting in an increase in the composition of Cu and Zn elements in the center area of generated plasma. Throughout this interval, the primary particles within the plasma's central region undergo a gradual transition from air components to components of the sample material. When the defocusing amount of the laser is positive, the vast majority of the laser energy is used to break down the air. In the generated plasma, the plasma generated on the sample surface at the edge of the plasma fluctuates greatly in the interaction process with the center plasma and environmental gas. Therefore, in this case, the emission spectra of the three elements H, N, and O obtained are relatively stable, while the emission spectra of the two elements Cu and Zn have poor stability. When the defocusing amount of the laser gradually becomes negative, the vast majority of the laser energy is used to excite the surface of the sample, making the central region of the plasma mainly composed of the sample components. During the interaction between the air components located at the edge of the plasma and the center plasma and environmental gas, there are large fluctuations. As a result, the stability of the emission spectra of the H, N, and O elements is poor.

Moreover, under different defocusing amounts, for the seven selected element spectrum lines, there is always a certain element's spectrum line stability about 5% . This phenomenon indicates that the plasma generated at different laser focusing depths is relatively stable. To verify this idea, the plasma morphology variation characteristics of the laser defocusing amount at relative positions ranging from 4 mm to -2 mm were studied, as shown in Figure 6.

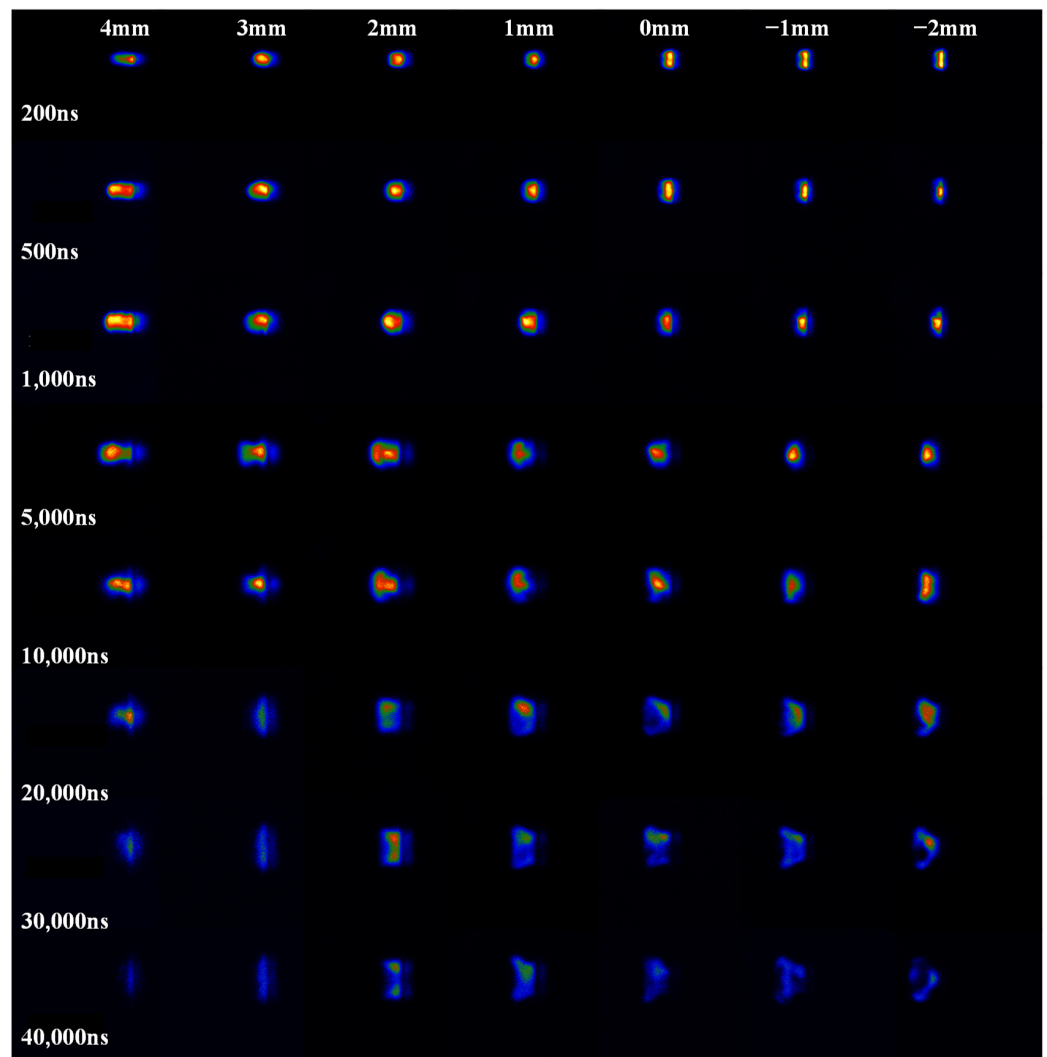


Figure 6. Temporal evolution of copper plasma morphology fluctuations under different laser defocus.

From Figure 6, it is found that the morphological changes in the plasma are relatively stable, without significant changes, despite varying depths of laser focus on the sample surface. In addition, within 500 ns after the plasma is generated, there is no plasma split [13]. When the plasma morphology is within 10,000 ns, the plasma main body morphology presents a good consistency without violent fluctuations. This phenomenon also confirms the stability of the above spectral collection. Between 10,000 ns~40,000 ns, the uniformity of the plasma morphology becomes worse.

In addition, there are significant differences in the evolution of plasma under different laser defocusing amounts. When the relative laser output delay is 200 ns and the laser focusing depth is 4 mm, the obtained plasma side profile is conical; when the laser is focused at a depth of 1 mm, the obtained plasma profile is circular; when the laser defocus is -2 mm, the obtained plasma profile is linear. In addition, when the relative laser output delay is 1000 ns and the laser focusing depth is 4 mm, the obtained plasma profile is approximately rectangular; at a laser focusing depth of 1 mm, the obtained plasma profile is approximately square in shape; when the laser defocus is -2 mm, the obtained plasma profile is approximately shuttle shaped. The reason for the significant difference in plasma morphology under different laser focusing depths may be that when the laser defocus is positive, the laser first penetrates the air and excites the sample. Due to the higher density of the sample plasma compared to the air plasma, a relatively thin gas environment is formed

in front of the generated sample plasma, which has a certain drag effect on the generated sample plasma. Therefore, as the plasma evolves over time, the lateral morphology will become longer. When the defocusing amount of the laser is negative, the laser beam directly excites the surface of the sample to produce plasma, without the drag effect of the thin gas environment. It only expands under the action of the plasma shock wave. Therefore, during the evolution process of the plasma, the length of the lateral morphology of the plasma does not change much. In order to explore the stability characteristics of spectra in different regions of plasma, the spectral stability of different defocusing amounts and collection positions was studied.

3.3. Collection Location and Spectral Stability

To investigate spectral line stability across various collection positions, the experiment recorded changes in spectral stability with a spectrometer delay of $1 \mu\text{s}$ and relative positions of spectrum collection ranging from 1 to 5, as depicted in Figure 2. Figure 7 illustrates the spectral line intensity and stability at different spectral acquisition positions when the laser is defocused by 4 mm.

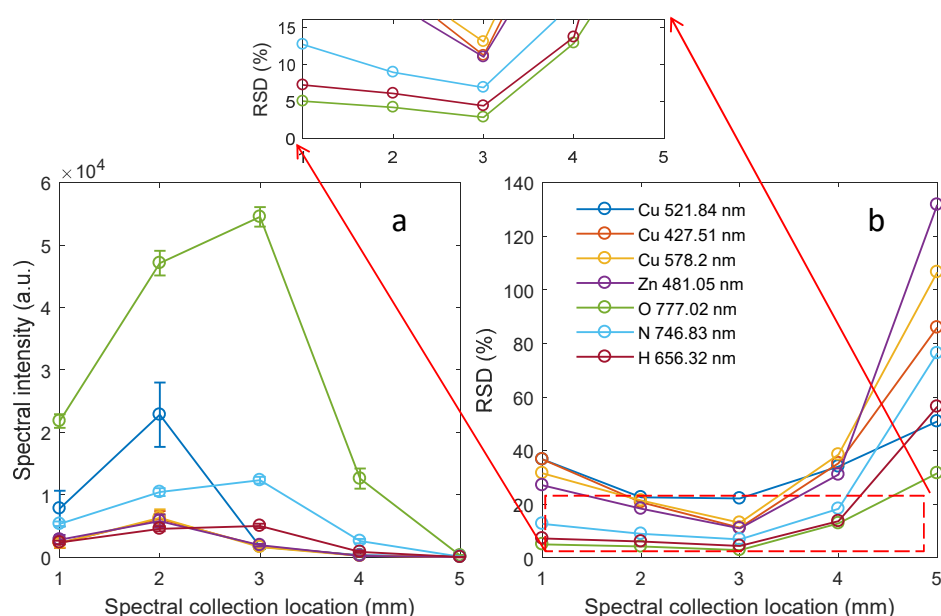


Figure 7. When the laser defocus is 4 mm, the spectral line intensity fluctuates in different spectral collection areas. Figures (a) and (b) respectively show the variation of the intensity and the relative standard deviation of spectral line with the spectral collection location. The error bars represent the standard deviation of the collected spectrum intensity.

From Figure 7a, the spectral line intensities of the detected elements Cu, Zn, O, N, and H all show a trend of first increasing and then decreasing. Among them, the spectral line intensities of Cu and Zn are the strongest at relative position 2, while the spectral line intensities of O, N, and H are the strongest at relative position 3. This indicates that when the laser is focused at a depth of 4 mm, the spectral acquisition delay is $1 \mu\text{s}$, and the integration time is $3 \mu\text{s}$, the region where the matrix element is located is mainly at position 2, and the region where the air plasma element is located is mainly at position 3. In addition, from Figure 7b, as the spectral collection positions change from 1 to 5, the relative standard deviations of the spectral line intensities corresponding to the elements Cu, Zn, O, N, and H show a trend of first weakening and then strengthening, and the relative standard deviations of the spectral lines obtained at position 3 are all the smallest. The reason for this phenomenon may be that in the early stage of plasma evolution, the position where the spectrum collection position 1 or 2 is located is the edge of the plasma. Due to the fact that particles in the edge region of the main plasma particles interact with both air and

the main plasma, the fluctuation of luminescent particles in the spectral collection area is relatively large. Therefore, the stability of the spectrum is relatively poor. In addition, when the relative position is 5, because the number of luminescent particles in the collected area is small, the effective spectrum is submerged in the spectrum background, and the stability of the obtained spectrum is poor. At the relative position 3, the spectrum collection position is in the central area of the plasma, and the overall density of the particles is relatively constant within the spectrum acquisition time range. The stability of the seven obtained spectral lines has been enhanced in this region, and the RSD of O 777.02 nm is 2.87%.

In order to explore the spectral stability of different focusing depths and collection positions, the changes in laser defocus between $-4\sim 4$ mm and the spectral stability collected at 1~5 spectral collection positions were analyzed. The relative standard deviations of the spectral line intensities of O and Cu elements obtained are shown in Tables 1 and 2, respectively.

Table 1. Relative standard deviation of O 777.02 nm.

Laser Defocus (mm)	Different Spectrum Collection Locations (mm)				
	1	2	3	4	5
4	5.03%	4.21%	2.87%	12.86%	31.56%
3	5.25%	2.35%	2.61%	26.05%	38.05%
2	5.88%	2.53%	4.85%	72.04%	37.39%
1	4.96%	2.96%	19.59%	38.52%	45.97%
0	5.12%	3.13%	32.31%	50.17%	53.28%
-1	6.48%	5.21%	32.94%	68.23%	70.66%
-2	5.35%	12.38%	54.24%	140.45%	117.34%
-3	10.92%	23.55%	92.82%	133.11%	162.54%
-4	15.91%	51.88%	173.01%	170.02%	160.75%

Table 2. Relative standard deviation of Cu 521.84 nm element.

Laser Defocus (mm)	Different Spectrum Collection Locations (mm)				
	1	2	3	4	5
4	36.73%	22.58%	22.14%	34.05%	50.90%
3	33.99%	29.31%	12.97%	78.66%	80.64%
2	22.23%	20.34%	14.02%	329.05%	31.67%
1	14.80%	11.38%	18.88%	27.61%	38.45%
0	8.72%	9.32%	49.02%	38.21%	39.81%
-1	6.11%	5.25%	23.20%	35.99%	38.68%
-2	4.32%	2.99%	19.00%	27.50%	37.64%
-3	3.22%	6.82%	17.00%	29.97%	26.87%
-4	5.11%	14.88%	21.98%	45.27%	42.01%

As shown in Table 1, the RSD changes in the O 777.02 nm at different spectral collection positions under different laser defocusing amounts are recorded. Experiments have found that as the defocusing amount of the laser decreases, the best collection position of the O 777.02 nm moves toward the direction of the sample. When the laser defocus is 4 mm, the most stable collection position for O element spectral lines is 3. However, when the laser defocus is $-1\sim 3$ mm, the most stable collection position for O element spectral line intensity obtained is 2. When the laser defocus is -2 , the most stable collection position for O element spectral lines obtained is 1.

Furthermore, for Cu 578.02 nm, the variation trend between the focusing depth of the laser on the sample surface and the optimal spectral acquisition position is not very obvious. When the laser is focused at a depth of 2 mm~4 mm on the sample surface, a relatively stable plasma emission signal can be obtained at the spectral acquisition position 3. When the laser is focused at a depth of 1 mm on the sample surface, a relatively stable spectral

signal acquisition position of 2 is obtained. When the focusing depth of the laser on the sample surface is 0, the acquisition position of the relatively stable spectral signal obtained is 1. When the laser focuses at a depth of -1 mm or -2 mm, a relatively stable plasma emission signal can be obtained at the spectral acquisition position 2. When the laser focuses at a depth of -3 mm or -4 mm, a relatively stable plasma emission signal can be obtained at the spectral acquisition position 1.

By comparing the stability of spectral lines corresponding to O and Cu elements, it has been partially verified that differences exist in the emission spectral lines of various elements within the spatial distribution of plasma. In addition, by comparing the data in Tables 1 and 2, as well as the plasma morphology captured in Figure 6, it can be observed that stable plasma emission spectral signals can be obtained near the plasma center region. When the focusing depth of the laser on the sample surface is negative, the center position of the plasma is approximately at the spectral acquisition position 1 or 2. Therefore, a relatively stable plasma emission spectrum signal can be obtained at the spectral acquisition position 1 or 2. When the laser focusing depth is positive, the obtained plasma center position is approximately at the spectral acquisition position 3, so a relatively stable plasma emission spectrum signal can also be obtained at that position.

4. Conclusions

In this paper, the effects of the laser's focus depth, the delay of the spectrometer, and the position of the spectrum collection on the spectral stability were carefully researched. Moreover, the dynamic characteristics of plasma were studied at different laser focusing depths. The study found that the uncertainty of the spectrum has a great relationship with the distribution of the main particles in the plasma, which is mainly reflected in the following two points:

- (1) In the initial stage of laser plasma generation, the collective behavior of the plasma leads to relatively small fluctuations in early particle behavior, resulting in the acquisition of a relatively stable spectrum. Moreover, research has found that the morphological changes in plasma are relatively stable, without significant changes, despite varying depths of laser focus on the sample surface. This finding suggests that LIBS can offer robust performance across different depths of analysis, enhancing its versatility and applicability in various fields.
- (2) The focal depth of the laser on the sample surface primarily influences the position distribution of the main particles within the plasma. Conducting spectrum collection near the central location of the plasma can yield a relatively stable spectrum, whereas the stability at the edges of the central location is lower.

Author Contributions: Conceptualization, methodology, software, investigation, data curation, funding acquisition, writing—original draft preparation and editing, W.W.; writing—review and editing, resources and data curation, L.S.; supervision, formal analysis, data curation, writing—review and editing, F.L. All authors have read and agreed to the published version of the manuscript.

Funding: This research was funded by the National Natural Science Foundation of China, grant number 42305152.

Institutional Review Board Statement: Not applicable.

Informed Consent Statement: Not applicable.

Data Availability Statement: Data are contained within the article.

Acknowledgments: Thank the LIBS team of Shenyang Institute of Automation, Chinese Academy of Sciences for their support on experimental equipment.

Conflicts of Interest: The authors declare no conflicts of interest.

References

1. Winefordner, J.D.; Gornushkin, I.B.; Correll, T.; Gibb, E.; Smith, B.W.; Omenetto, N. Comparing several atomic spectrometric methods to the super stars: Special emphasis on laser induced breakdown spectrometry, LIBS, a future super star. *J. Anal. At. Spectrom.* **2004**, *19*, 1061–1083. [[CrossRef](#)]
2. Hahn, D.W.; Omenetto, N. Laser-Induced Breakdown Spectroscopy (LIBS), Part I: Review of Basic Diagnostics and Plasma-Particle Interactions: Still-Challenging Issues Within the Analytical Plasma Community. *Appl. Spectrosc.* **2010**, *64*, 335A–366A. [[CrossRef](#)] [[PubMed](#)]
3. Hahn, D.W.; Omenetto, N. Laser-Induced Breakdown Spectroscopy (LIBS), Part II: Review of Instrumental and Methodological Approaches to Material Analysis and Applications to Different Fields. *Appl. Spectrosc.* **2012**, *66*, 347–419. [[CrossRef](#)] [[PubMed](#)]
4. Afgan, M.S.; Hou, Z.Y.; Song, W.R.; Liu, J.; Song, Y.; Gu, W.; Wang, Z. On the Spectral Identification and Wavelength Dependence of Rare-Earth Ore Emission by Laser-Induced Breakdown Spectroscopy. *Chemosensors* **2022**, *10*, 350. [[CrossRef](#)]
5. Noll, R.; Fricke-Begemann, C.; Brunk, M.; Connemann, S.; Meinhardt, C.; Scharun, M.; Sturm, V.; Makowe, J.; Gehlen, C. Laser-induced breakdown spectroscopy expands into industrial applications. *Spectrochim. Acta Part B At. Spectrosc.* **2014**, *93*, 41–51. [[CrossRef](#)]
6. Rezaei, F.; Cristoforetti, G.; Tognoni, E.; Legnaioli, S.; Palleschi, V.; Safi, A. A review of the current analytical approaches for evaluating, compensating and exploiting self-absorption in Laser Induced Breakdown Spectroscopy. *Spectrochim. Acta Part B At. Spectrosc.* **2020**, *169*, 105878. [[CrossRef](#)]
7. Takahashi, T.; Thornton, B. Quantitative methods for compensation of matrix effects and self-absorption in Laser Induced Breakdown Spectroscopy signals of solids. *Spectrochim. Acta Part B At. Spectrosc.* **2017**, *138*, 31–42. [[CrossRef](#)]
8. Motto-Ros, V.; Syvilay, D.; Bassel, L.; Negre, E.; Trichard, F.; Pelascini, F.; El Haddad, J.; Harhira, A.; Moncayo, S.; Picard, J.; et al. Critical aspects of data analysis for quantification in laser-induced breakdown spectroscopy. *Spectrochim. Acta Part B At. Spectrosc.* **2018**, *140*, 54–64. [[CrossRef](#)]
9. Multari, R.A.; Foster, L.E.; Cremers, D.A.; Ferris, M.J. Effect of Sampling Geometry on Elemental Emissions in Laser-Induced Breakdown Spectroscopy. *Appl. Spectrosc.* **1996**, *50*, 1483–1499. [[CrossRef](#)]
10. Wisbrun, R.; Schechter, I.; Niessner, R.; Schroeder, H.; Kompa, K.L. Detector for trace elemental analysis of solid environmental samples by laser-plasma spectroscopy. *Anal. Chem.* **1994**, *66*, 2964–2975. [[CrossRef](#)]
11. Aguilera, J.; Aragón, C.; Peñalba, F. Plasma shielding effect in laser ablation of metallic samples and its influence on LIBS analysis. *Appl. Surf. Sci.* **1998**, *127–129*, 309–314. [[CrossRef](#)]
12. Harilal, S.S.; Bindhu, C.V.; Tillack, M.S.; Najmabadi, F.; Gaeris, A.C. Internal structure and expansion dynamics of laser ablation plumes into ambient gases. *J. Appl. Phys.* **2003**, *93*, 2380–2388. [[CrossRef](#)]
13. Wen, S.-B.; Mao, X.; Greif, R.; Russo, R.E. Expansion of the laser ablation vapor plume into a background gas. I. Analysis. *J. Appl. Phys.* **2007**, *101*, 023114. [[CrossRef](#)]
14. Wen, S.-B.; Mao, X.; Greif, R.; Russo, R.E. Laser ablation induced vapor plume expansion into a background gas. II. Experimental analysis. *J. Appl. Phys.* **2007**, *101*, 023115. [[CrossRef](#)]
15. Fu, Y.-T.; Gu, W.-L.; Hou, Z.-Y.; Muhammed, S.A.; Li, T.-Q.; Wang, Y.; Wang, Z. Mechanism of signal uncertainty generation for laser-induced breakdown spectroscopy. *Front. Phys.* **2020**, *16*, 22502. [[CrossRef](#)]
16. Fu, Y.; Hou, Z.; Li, T.; Li, Z.; Wang, Z. Investigation of intrinsic origins of the signal uncertainty for laser-induced breakdown spectroscopy. *Spectrochim. Acta Part B At. Spectrosc.* **2019**, *155*, 67–78. [[CrossRef](#)]
17. Russo, R.E.; Mao, X.L.; Liu, C.; Gonzalez, J. Laser assisted plasma spectrochemistry: Laser ablation. *J. Anal. At. Spectrom.* **2004**, *19*, 1084–1089. [[CrossRef](#)]
18. Russo, R.E. Laser Ablation. *Appl. Spectrosc.* **1995**, *49*, 14A–28A. [[CrossRef](#)]

Disclaimer/Publisher’s Note: The statements, opinions and data contained in all publications are solely those of the individual author(s) and contributor(s) and not of MDPI and/or the editor(s). MDPI and/or the editor(s) disclaim responsibility for any injury to people or property resulting from any ideas, methods, instructions or products referred to in the content.